Eur. Phys. J. D **7**, 249–254 (1999)

THE EUROPEAN PHYSICAL JOURNAL D

EDP Sciences

Orientation phenomena for electron-ion collisional excitations in strongly coupled plasmas

Young-Dae Jung[a]

Department of Physics, Hanyang University, Ansan, Kyunggi-Do 425-791, South Korea

Received: 16 December 1998 / Received in final form: 23 March 1999

Abstract. In strongly coupled plasmas, the orientation phenomena for direct $1s \rightarrow 2p_{\pm 1}$ excitations in electron-hydrogenic ion collisions are investigated using the ion-sphere interaction potential. For small impact parameters, the orientation parameters have minima which correspond to the complete $1s \rightarrow 2p_{-1}$ transitions. The target screening effects slightly increase the probability of populating the $2p_{-1}$ state.

PACS. 52.20.Fs Electron collisions

1 Introduction

Electron-ion collisions [1–6] in plasmas have been extensively studied in recent years since these processes can be used for plasma diagnostics. The orientation and alignment phenomena in electron-atom and electron-ion collisions have been actively investigated, since these phenomena provide detailed information on the mechanism of collisional excitation of target atoms and ions [7–9]. A recent experimental investigation shows the possibility of the detection of radiative transitions from the excited $p_{\pm 1}(m = \pm 1)$ states to the ground state [10]. The orientation phenomena in plasmas could provide detailed information about the plasma parameters. The orientation phenomena for *s*-*p* electron-ion excitations in weakly coupled plasmas [11,12] have been investigated using the non-spherical Debye-Hückel model. It has been found that the plasma-screening effect appreciably reduces a favoring of the $s \rightarrow p_{-1}$ transition for high-energy projectiles. However, the orientation phenomena in strongly coupled plasmas have not been investigated. A most typical example of strongly coupled classical plasma may be seen in the system of ions inside a highly evolved star [13]. Thus, in this paper we investigate the orientation phenomena for direct $1s \rightarrow 2p_{\pm 1}$ electron-ion excitations in strongly coupled plasmas using the ion-sphere model. The ion-sphere model [14,15] has played an important part in elucidating the properties of the strongly coupled plasma. The ion-sphere model has been widely used to investigate the atomic processes in strongly coupled plasmas, such as elastic [16] and inelastic [3] collision processes. The ion-sphere model is also applied to the electron capture processes from hydrogenic ions by fully stripped ions in strongly coupled plasmas [17]. Recently, bremsstrahlung in electron-ion Coulomb scattering in strongly coupled plasmas was investigated using the ion-sphere model with the hyperbolic-orbit trajectory method [18]. Thus, we use an appropriate form of the ion-sphere model to represent the interaction between the projectile electron and target ion in strongly coupled plasmas. In this paper, we use the semiclassical straight-line (SL) trajectory method [2, 19] to describe the motion of the projectile electron and to visualize the plasma-screening effect on the orientation parameters. The screened wave functions and energies of the target ion in strongly coupled plasmas are obtained by the Ritz variation method [20]. The orientation parameters ($L_\perp$) [8,11,12] for direct $1s \rightarrow 2p_{\pm 1}$ excitations are obtained as functions of the impact parameter (b) and ion-sphere radius (R_Z). The results show that the probability of populating the $2p_{-1}$ state tends to dominate over the probability of populating the $2p_{+1}$ state in planar collisions, due to a propensity rule [8]. The probability of populating the $2p_{-1}$ state is increased with an increase of the projectile energy. However, near the ion-sphere boundary ($b \approx R_Z$), the probability of populating the $2p_{-1}$ state is almost equal to that of populating the $2p_{+1}$ state, *i.e.*, $L_\perp \approx 0$. For small impact parameter domain, the orientation parameters have minima which correspond to the complete $1s \rightarrow 2p_{-1}$ transitions since the $1s \rightarrow 2p_{+1}$ transition probabilities are quite small for $b < a_Z$, where a_Z ($\equiv a_0/Z = \hbar^2/Zme^2$) is the Bohr radius of a hydrogenic ion with nuclear charge Z. The plasma-screening effect on the bound electron in target ion slightly increases a favoring of the $1s \rightarrow 2p_{-1}$ transition. It is also found that the target screening effects are more important for the case of the small ion-sphere radius and slightly increased with increasing the projectile energy. These results provide a general description of the orientation phenomena for *s*-*p* excitation in strongly coupled plasmas.

In section 2, we derive a closed form of the semiclassical transition amplitude for direct $1s \rightarrow 2p_{\pm 1}$ excitations in electron-hydrogenic ion collisions in strongly coupled

[a] e-mail: yjung@bohr.hanyang.ac.kr

plasmas using the ion-sphere model and the semiclassical SL path approximation. In section 3, we obtain the screened wave functions and energies of the bound electron in target ion using the Ritz variation method. In section 4, we obtain the transition probabilities and orientation parameters for direct $1s \rightarrow 2p_{\pm1}$ excitations as functions of the impact parameter and ion-sphere radius. We also investigate the variation of the orientation parameter with a change of the projectile energy and ion-sphere radius. Finally, in section 5, a summary and discussion are given.

2 Transition amplitudes for $1s \rightarrow 2p_{\pm1}$ excitations

From a first-order semiclassical approximation, the cross-section [21] for excitation from an unperturbed atomic state $|n\rangle[\equiv \Psi_{nlm}(\mathbf{r})]$ to an excited state $|n'\rangle[\equiv \Psi_{n'l'm'}(\mathbf{r})]$ is given by

$$\sigma_{n',n} = 2\pi \int b\, \mathrm{d}b \left|T_{n',n}(b)\right|^2, \tag{1}$$

where b is the impact parameter and $T_{n',n}(b)$ is the transition amplitude,

$$T_{n',n} = -\frac{i}{\hbar}\int_{-\infty}^{\infty} \mathrm{d}t\, e^{i\omega_{n',n}t}\langle n'|V(\mathbf{r},\mathbf{R})|n\rangle\,, \tag{2}$$

where $\omega_{n',n} \equiv (E_{n'} - E_n)/\hbar$, and E_n and $E_{n'}$ are the energies of atomic states n and n', respectively. This semiclassical impact parameter method has a strong appeal in aiding the physical intuition. Usually, calculations based on this method are mathematically more tractable than fully quantum-mechanical treatments.

In strongly coupled plasmas, the Debye number becomes smaller than unity; the concept of Debye screening as a cooperative phenomenon is no longer applicable. The probability of finding other charged particles in a Debye sphere almost vanishes. Hence, the Debye-Hückel model is not reliable to describe the interaction potential in strongly coupled plasmas. To understand salient features of such a strongly coupled plasma, it is instructive to introduce the ion-sphere model [14]. It is equivalent to the Wigner-Seitz sphere used in condensed-matter theory. The ion-sphere consists of a single ion and its surrounding negative-charge sphere. For simplicity, we assume that the target is a hydrogenic ion target with nuclear charge Z placed in a strongly coupled plasma. Then, the interaction potential $V(\mathbf{r},\mathbf{R})$ obtained by the ion-sphere model [14, 16] becomes

$$V(\mathbf{r},\mathbf{R}) = \left(-\frac{Ze^2}{R} + \frac{e^2}{|\mathbf{R}-\mathbf{r}|}\right) \times \left[1 - \frac{R}{2R_Z}\left(3 - \frac{R^2}{R_Z^2}\right)\right]\theta(R_Z - R), \tag{3}$$

where $\mathbf{r}$ and $\mathbf{R}$ are the positions of the bound electron and the projectile electron, respectively, and $\theta(x)$ ($= 1$ for $x \geq 0$; $= 0$ for $x < 0$) is the step function. The ion-sphere radius R_Z is given by the plasma electron density n_e,

$$R_Z = [3(Z-1)/4\pi n_\mathrm{e}]^{1/3}, \tag{4}$$

since the total charge within the sphere is neutral. This ion-sphere potential (Eq. (3)) is designed so that potential and its first derivative vanish at the ion-sphere radius. Thus, in strongly coupled plasmas, screening is better described by this ion-sphere picture, in which the stationary hydrogenic ion of total charge $Z-1$ is surrounded by $Z-1$ electrons, uniformly distributed throughout the ion-sphere radius.

For electron-impact excitation processes ($n \neq n'$), *i.e.*, inelastic collisions, the electron-nucleus interaction term does not contribute to the transition amplitude due to orthogonality of the initial and final states of the target system. Then the transition amplitudes for $1s \rightarrow 2p_{\pm1}$ ($m = \pm1$) excitations become

$$T_{2p_{\pm1},1s} = -\frac{ie^2}{\hbar}\int_{-\infty}^{\infty} \mathrm{d}t\, e^{i\omega_{2p_{\pm1},1s}t/\hbar} \times \left[1 - \frac{R}{2R_Z}\left(3 - \frac{R^2}{R_Z^2}\right)\right]\overline{V}_{2p_{\pm1},1s}, \tag{5}$$

where $\overline{V}_{2p_{\pm1},1s}$ are the transition matrix elements

$$\overline{V}_{2p_{\pm1},1s} = \int \mathrm{d}^3\,\mathbf{r}\Psi^*_{2p_{\pm1}}(\mathbf{r})\frac{1}{|\mathbf{R}-\mathbf{r}|}\Psi_{1s}(\mathbf{r}). \tag{6}$$

Using the addition theorem [22] with spherical harmonics Y_{lm}:

$$\frac{1}{|\mathbf{R}-\mathbf{r}|} = \sum_{l=0}^{\infty}\sum_{m=-l}^{l}\frac{4\pi}{2l+1}\frac{r_<^l}{r_>^{l+1}}Y_{lm}(\hat{r})Y^*_{lm}(\widehat{R}), \tag{7}$$

where $r_<(r_>)$ is the lesser (greater) of r and R, the transition matrix elements can be written as

$$\overline{V}_{2p_{\pm1},1s} = \frac{\sqrt{4\pi}}{3}Y^*_{1\pm1}(\widehat{R}) \times \left[\frac{1}{R^2}\int_0^R r^3\mathrm{d}r R_{2p}(r)R_{1s}(r) + R\int_R^{R_Z}\mathrm{d}r\, R_{2p}(r)R_{1s}(r)\right], \tag{8}$$

where $R_{1s}(r)$ and $R_{2p}(r)$ are the radial $1s$ and $2p$ target wave functions, respectively. The plasma-screening effects on these radial wave functions will be discussed in section 4. The first term in equation (8) vanishes in the long-range dipole approximation ($R > r$). However, we shall keep this term to investigate the close-encounter effect [12] on the transition amplitudes and orientation parameters for small impact parameters.

3 Atomic wave functions and energies

3.1 Schrödinger equation

When an atom is embedded in plasmas, its wave functions and energies are different from those of a free atom because

the nucleus is shielded by the surrounding plasma. Then, the radial Schrödinger equation for a hydrogenic ion with nuclear charge Z in uniformly distributed strongly coupled plasmas would be given by

$$\left[-\frac{\hbar^2}{2m}\left(\frac{\mathrm{d}^2}{\mathrm{d}r^2}-\frac{l(l+1)}{r^2}\right)-\frac{Z_{nl}e^2}{r}\right]P_{nl}(r)=E_{nl}P_{nl}(r), \quad (9)$$

where $P_{nl}(r)$ and E_{nl} are the radial wave function and the energy of the nl-th shell electron. Here Z_{nl} is the effective charge of the nl-th shell electron:

$$Z_{nl}=Z-\delta_{nl}(Z,R_Z), \quad (10)$$

where the screening constant $\delta_{nl}(Z,R_Z)$ is determined by the surrounding plasma electrons within the nl-th shell effective Bohr radius $n^2a_{Z_{nl}}$ ($\equiv n^2a_0/Z_{nl}$):

$$\delta_{nl}(Z,R_Z)=4\pi\int_0^{n^2a_{Z_{nl}}} r^2\,\mathrm{d}r\,n_\mathrm{e}(R_Z). \quad (11)$$

Here we consider a simple analytic method to obtain the solutions of equation (9) because the simple analytic solutions are, of course, more convenient to use for calculating the transition matrix elements. The normalized trial $1s$ and $2p$ wave functions are given, respectively, as follows:

$$P_{1s}(r)\equiv rR_{1s}(r)=2\alpha_{1s}^{-3/2}re^{-r/\alpha_{1s}}, \quad (12)$$

$$P_{2p}(r)\equiv rR_{2p}(r)=\frac{1}{2\sqrt{6}}\alpha_{2p}^{-5/2}r^2e^{-r/2\alpha_{2p}}, \quad (13)$$

where α_{1s} and α_{2p} are the $1s$ and $2p$ variation parameters and $\alpha_{1s}=\alpha_{2p}\to a_Z$ for vanishing plasma screening effects ($R_Z\to\infty$). These parameters will be determined in the following sections.

3.2 Ground (1s) state

The expectation value of the ground-state energy is given by equations (9) and (12):

$$\langle E_{1s}(\alpha_{1s})\rangle=\frac{\hbar^2}{2m\alpha_{1s}^2}-\frac{(Z-\delta_{1s})e^2}{\alpha_{1s}}. \quad (14)$$

Here the parameter α_{1s} is obtained from the minimization of $\langle E_{1s}(\alpha_{1s})\rangle$, *i.e.*, $\partial\langle E_{1s}(\alpha_{1s})\rangle/\partial\alpha_{1s}=0$:

$$\alpha_{1s}=\frac{a_Z}{1-\delta_{1s}/Z}. \quad (15)$$

From equations (4) and (11) and using the perturbation method since $\delta_{1s}<Z$, the $1s$ screening constant δ_{1s} is found to be

$$\delta_{1s}\cong\frac{(Z-1)(a_Z/R_Z)^3}{1-3(1-1/Z)(a_Z/R_Z)^3}. \quad (16)$$

Then the approximate solution for α_{1s} is

$$\alpha_{1s}\cong\eta_{1s}a_Z, \quad (17)$$

where $\eta_{1s}^{-1}\equiv1-(1-1/Z)(a_Z/R_Z)^3$. Here η_{1s} represents the plasma-screening effect on the ground state. Then, the ground-state energy is obtained from equations (14) and (15):

$$\langle E_{1s}\rangle=-\frac{(Z-\delta_{1s})e^2}{2\alpha_{1s}}. \quad (18)$$

3.3 Excited (2p) state

As in the previous section, the expectation value of the $2p$ state energy is given by equations (9) and (13):

$$\langle E_{2p}(\alpha_{2p})\rangle=\frac{\hbar^2}{8m\alpha_{2p}^2}-\frac{(Z-\delta_{2p})e^2}{4\alpha_{2p}}. \quad (19)$$

The parameter α_{2p} is also obtained from the minimization of $\langle E_{2p}(\alpha_{2p})\rangle$, *i.e.*, $\partial\langle E_{2p}(\alpha_{2p})\rangle/\partial\alpha_{2p}=0$:

$$\alpha_{2p}=\frac{a_Z}{1-\delta_{2p}/Z}. \quad (20)$$

From equations (4) and (11) and also using the perturbation method, the $2p$ screening constant δ_{2p} is given by

$$\delta_{2p}\cong\frac{(Z-1)(4a_Z/R_Z)^3}{1-3(1-1/Z)(4a_Z/R_Z)^3}. \quad (21)$$

Then the approximate solution for α_{2p} becomes

$$\alpha_{2p}\cong\eta_{2p}a_Z, \quad (22)$$

where $\eta_{2p}^{-1}\equiv1-(1-1/Z)(4a_Z/R_Z)^3$. Here η_{2p} represents the target screening effect on the $2p$ excited state. The $2p$ state energy can also be obtained from equations (19) and (20):

$$\langle E_{2p}\rangle=-\frac{(Z-\delta_{2p})e^2}{8\alpha_{2p}}. \quad (23)$$

4 Orientation parameters

From equations (8), (12), (13), (17), and (22), the $1s\to2p_{\pm1}$ transition matrix elements $\overline{V}_{2p_{\pm1},1s}$ are given by

$$\overline{V}_{2p_{\pm1},1s}=\frac{8\sqrt{6\pi}}{3}\,\frac{\eta_{1s}^{-3/2}\eta_{2p}^{-5/2}}{\beta^2a_Z^4}\,\frac{Y_{1\pm1}^*(\widehat{R})}{R^2}\times\left[1-\left(1+\beta R+\frac{1}{2}\beta^2R^2+\frac{1}{8}\beta^3R^3\right)\times e^{-\beta R}-\frac{1}{24}\beta^3R^3(1+\beta R_Z)e^{-\beta R_Z}\right], \quad (24)$$

where $\beta a_Z\equiv\eta_{1s}^{-1}+(2\eta_{2p})^{-1}$.

To describe the projectile motion, we assume that the projectile electron is moving on a SL trajectory in the so-called natural coordinate frame [8,12] in which the axis

of quantization z is chosen perpendicular to the collision plane. Then the position of the projectile electron can be written as a function of time t and the impact parameter b,

$$\mathbf{R}(t) = vt\hat{x} + b\hat{y}, \tag{25}$$

where v is the velocity of the projectile electron. Here $t = 0$ is arbitrarily chosen as the instant at which the projectile electron makes its closest approach to the target ion. Under these circumstances, in $1s \rightarrow 2p$ excitation, conservation law prohibits the $1s \rightarrow 2p_0$ ($m = 0$) transition; only $m = \pm 1$ substates ($2p_{\pm 1}$) of the $2p$ level are possible. In this natural coordinate frame, the spherical harmonic $Y^*_{1\pm1}(\widehat{R})$ becomes

$$Y^*_{1\pm1}(\widehat{R}) = \mp\sqrt{\frac{3}{8\pi}}\frac{(vt \mp ib)}{R}. \tag{26}$$

Then, the $T_{2p_{\pm1},1s}$ transition amplitudes without using the dipole approximation become

$$\begin{aligned} T_{2p_{\pm1},1s} = \pm\frac{4ie^2}{\hbar}\frac{\eta_{1s}^{-3/2}\eta_{2p}^{-5/2}}{\beta^2 a_Z^4} \\ \times \int_{-t_Z}^{t_Z} \mathrm{d}t\, e^{i\omega_{\pm}t}\frac{(vt \mp ib)}{R^3}\left(1 - \frac{3R}{2R_Z} + \frac{R^3}{2R_Z^3}\right) \\ \times\Bigg[1 - \left(1 + \beta R + \frac{1}{2}\beta^2R^2 + \frac{1}{8}\beta^3R^3\right) \\ \times e^{-\beta R} - \frac{1}{24}\beta^3R^3(1 + \beta R_Z)e^{-\beta R_Z}\Bigg], \end{aligned} \tag{27}$$

where $t_Z = (R_Z^2 - b^2)^{1/2}/v$ due to the cutoff radius R_Z of the ion-sphere model and $\omega_{\pm}\,(\equiv \omega_{2p_{\pm1},1s}) = e^2\Delta/\hbar a_Z$ with

$$\Delta = -\frac{(Z - \delta_{2p})}{8\eta_{2p}} + \frac{(Z - \delta_{1s})}{2\eta_{1s}}. \tag{28}$$

Here we introduce the dimensionless time $\tau\,(\equiv vt/a_Z)$ and the scaled kinetic energy of the incident electron $\varepsilon\,(\equiv mv^2/2Z^2Ry)$, then the transition amplitudes $T_{\pm}$ ($\equiv T_{2p_{\pm1},1s}$) including the target screening effects are found to be

$$\begin{aligned} T_{\pm}^{\mathrm{S}}(\bar{b}, \overline{R}_Z, Z, \varepsilon) = \mp\frac{8\eta_{1s}^{-3/2}\eta_{2p}^{-5/2}}{\overline{\beta}^5 Z\sqrt{\varepsilon}} \\ \times \int_0^{\sqrt{\overline{R}_Z^2 - \bar{b}^2}} \mathrm{d}\tau \frac{\tau\sin\left(\dfrac{\Delta\tau}{Z\sqrt{\varepsilon}}\right) \mp \bar{b}\cos\left(\dfrac{\Delta\tau}{Z\sqrt{\varepsilon}}\right)}{\overline{R}^3} \\ \times\left(1 - \frac{3\overline{R}}{2\overline{R}_Z} + \frac{\overline{R}^3}{2\overline{R}_Z^3}\right) \\ \times\Bigg[1 - \left(1 + \overline{\beta}\,\overline{R} + \frac{1}{2}\overline{\beta}^2\overline{R}^2 + \frac{1}{8}\overline{\beta}^3\overline{R}^3\right) \\ \times e^{-\overline{\beta}\overline{R}} - \frac{1}{24}\overline{\beta}^3\overline{R}^3(1 + \overline{\beta}\,\overline{R}_Z)e^{-\overline{\beta}\,\overline{R}_Z}\Bigg], \end{aligned} \tag{29}$$

where $\overline{\beta}\,(\equiv \beta a_Z) = \eta_{1s}^{-1} + (2\eta_{2p})^{-1}$, $\overline{R} = \sqrt{\bar{b}^2 + \tau^2}$, $\overline{R}_Z$ ($\equiv R_Z/a_Z$) is the scaled ion-sphere radius, and $\bar{b}\,(\equiv b/a_Z)$ is the scaled impact parameter. If we neglect the target screening effects, *i.e.*, $\eta_{1s} = \eta_{2p} \rightarrow 1$, $\overline{\beta} \rightarrow 3/2$, and $\Delta \rightarrow 3Z/8$, the transition amplitudes become

$$\begin{aligned} T_{\pm}^{\mathrm{NS}}(\bar{b}, \overline{R}_Z, Z, \varepsilon) = \mp\frac{2^8}{3^5 Z\sqrt{\varepsilon}} \\ \times \int_0^{\sqrt{\overline{R}_Z^2 - \bar{b}^2}} \mathrm{d}\tau \frac{\tau\sin\left(\dfrac{3\tau}{8\sqrt{\varepsilon}}\right) \mp \bar{b}\cos\left(\dfrac{3\tau}{8\sqrt{\varepsilon}}\right)}{\overline{R}^3} \\ \times\left(1 - \frac{3\overline{R}}{2\overline{R}_Z} + \frac{\overline{R}^3}{2\overline{R}_Z^3}\right) \\ \times\Bigg[1 - \left(1 + \frac{3}{2}\overline{R} + \frac{9}{8}\overline{R}^2 + \frac{27}{64}\overline{\beta}^3\overline{R}^3\right) \\ \times e^{-3\overline{R}/2} - \frac{9}{64}\overline{R}^3\left(1 + \frac{3}{2}\overline{R}_Z\right)e^{-3\overline{R}_Z/2}\Bigg]. \end{aligned} \tag{30}$$

The orientation parameter is defined as

$$\begin{aligned} L_{\perp}(\bar{b}, \overline{R}_Z, Z, \varepsilon) = \\ \frac{|T_+(\bar{b}, \overline{R}_Z, Z, \varepsilon)|^2 - |T_-(\bar{b}, \overline{R}_Z, Z, \varepsilon)|^2}{|T_+(\bar{b}, \overline{R}_Z, Z, \varepsilon)|^2 + |T_-(\bar{b}, \overline{R}_Z, Z, \varepsilon)|^2}. \end{aligned} \tag{31}$$

This quantity $L_{\perp}(\bar{b}, \overline{R}_Z, Z, \varepsilon)$ is a measure of the expectation value of the transferred orbital angular momentum to the bound electron in target ion due to the direct $1s \rightarrow 2p_{\pm1}$ excitations. Since the line intensity ratios are directly related to the $1s \rightarrow 2p_{\pm1}$ excitation rates [23], the orientation parameter is connected to the relative number of coincidences for RHC (right-hand circularly polarized light) and LHC (left-hand circularly polarized light) photons emitting due to the radiative decay from the excited $2p_{-1}$ and $2p_{+1}$ states to the ground 1s state.

In order to explicitly investigate the orientation parameter for direct electron-ion excitations, we consider the hydrogenic ion target with nuclear charge $Z = 10$. Here we consider three cases of the ion-sphere: $\overline{R}_Z = 10$, 20, and 40 and two cases of the projectile energies: $\varepsilon = 9$ and 25 since the semiclassical SL trajectory method is known to be valid for the high-energy condition $\varepsilon > 7$ [24]. Figure 1 shows the orientation parameters for direct $1s \rightarrow 2p_{\pm1}$ excitations as functions of the scaled impact parameter and ion-sphere radius. The probability of populating the $2p_{-1}$ state dominates the probability of populating the $2p_{+1}$ state in planar collisions, due to a propensity rule. However, for large impact parameter domain, *i.e.*, near the ion-sphere boundary, the probability of populating the $2p_{-1}$ state is almost equal to that of populating the $2p_{+1}$ state, *i.e.*, $L_{\perp} \approx 0$. The probability of populating the $2p_{-1}$ state is increased with an increase of the projectile energy. For small impact parameter domain, the orientation parameters have minima which correspond to the complete $1s \rightarrow 2p_{-1}$ transitions since the $1s \rightarrow 2p_{+1}$

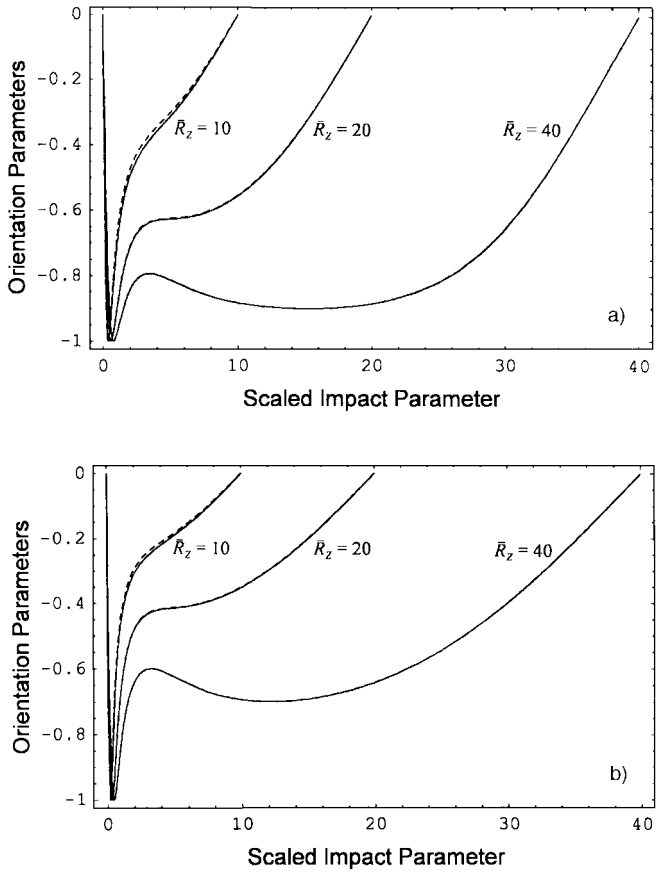

Fig. 1. The orientation parameters $L_\perp(\bar{b}, \overline{R}_Z, Z, \varepsilon)$ for direct $1s \rightarrow 2p_{\pm 1}$ excitations for $\overline{R}_Z = 10$, 20, and 40. The solid lines represent the orientation parameters including the target screening effects. The dashed lines represent the orientation parameters neglecting the target screening effects. ((a) $\varepsilon = 9$; (b) $\varepsilon = 25$.)

Table 1. The orientation parameters $L_\perp(\bar{b}, \overline{R}_Z, Z, \varepsilon)$ for direct $1s \rightarrow 2p_{\pm 1}$ excitations at $\bar{b}_{1/2}\,(\equiv \overline{R}_Z/2)$ for $\varepsilon = 9$.

$\overline{R}_Z$	$L_\perp^{\rm S}(\varepsilon = 9)^{\rm a}$	$L_\perp^{\rm NS}(\varepsilon = 9)^{\rm b}$
10	−0.3120 (at $\bar{b} = 5$)	−0.3004 (at $\bar{b} = 5$)
20	−0.5566 (at $\bar{b} = 10$)	−0.5545 (at $\bar{b} = 10$)
40	−0.8860 (at $\bar{b} = 20$)	−0.8858 (at $\bar{b} = 20$)

[a] The orientation parameters given by equations (29) and (31) (including the target screening effects).

[b] The orientation parameters given by equations (30) and (31) (neglecting the target screening effects).

Table 2. The orientation parameters $L_\perp(\bar{b}, \overline{R}_Z, Z, \varepsilon)$ for direct $1s \rightarrow 2p_{\pm 1}$ excitations at $\bar{b}_{1/2}\,(\equiv \overline{R}_Z/2)$ for $\varepsilon = 25$.

$\overline{R}_Z$	$L_\perp^{\rm S}(\varepsilon = 25)^{\rm a}$	$L_\perp^{\rm NS}(\varepsilon = 25)^{\rm b}$
10	−0.1900 (at $\bar{b} = 5$)	−0.1823 (at $\bar{b} = 5$)
20	−0.3523 (at $\bar{b} = 10$)	−0.3508 (at $\bar{b} = 10$)
40	−0.6426 (at $\bar{b} = 20$)	−0.6423 (at $\bar{b} = 20$)

[a] The orientation parameters given by equations (29) and (31) (including the target screening effects).

[b] The orientation parameters given by equations (30) and (31) (neglecting the target screening effects).

transition probabilities are quite small for $\bar{b} < 1$. Recently, these phenomena were also found in weakly coupled plasmas described by the Debye-Hückel model including the close-encounter effects [12]. Since the orientation parameter (Eq. (31)) is obtained by the transition amplitudes (Eq. (27)) including the close-encounter effects, *i.e.*, without using the dipole approximation, the results for small impact parameter domain would be quite reliable. It has been known that the behavior of the orientation parameters using the dipole approximation, *i.e.*, neglecting the close-encounter effects is quite different from that including the close-encounter effects [11]. A recent investigation [12] shows that the close-encounter effects are quite useful to investigate the behavior of the transition probabilities for small impact parameters. The minima phenomena [25] are also found in the Lorentzian distribution plasma for all values of the spectral index κ including the close-encounter effects. Numerical values of the orientation parameters at the midpoint $\bar{b}_{1/2}\,(\equiv \overline{R}_Z/2)$ are listed in Tables 1 and 2. As we see in these tables, the plasma-screening effects on the bound electron in target ion slightly increase the probability of populating the $2p_{-1}$ state. It is worth noting that the target screening effects are more important for the case of the small ion-sphere radius (*e.g.*, $\cong$ 3.9% for $\overline{R}_Z = 10$ and $\varepsilon = 9$, $\cong$ 0.4% for $\overline{R}_Z = 20$ and $\varepsilon = 9$) and also slightly increased with increasing the projectile energy. Recently, there has been an experimental evidence [10] for detecting the relative number of coincidences for RHC and LHC photons from atom-ion collisional excitations. So, in the future, we may detect and resolve the relative number of RHC and LHC photons due to the $1s \rightarrow 2p_{\pm 1}$ electron-ion excitations in strongly coupled plasmas.

5 Summary and discussion

In this paper, we investigate the orientation phenomena for direct electron-hydrogenic ion collisions in strongly coupled plasmas using the ion-sphere interaction potential. The semiclassical straight-line trajectory method is applied to treat the projectile electron as a classical point particle and the target wave functions are obtained using the Ritz variation method. Without using the dipole

approximation, the orientation parameter for direct $1s \rightarrow 2p_{\pm 1}$ excitation is obtained as a function of the impact parameter and ion-sphere radius. The results show that the probability of populating the $2p_{-1}$ state tends to dominate over the probability of populating the $2p_{+1}$ state in planar collisions in the natural coordinate frame. However, for large impact parameter domain the probability of populating the $2p_{-1}$ state is almost equal to that of populating the $2p_{+1}$ state so that the orientation parameter becomes zero. It is also found that the probability of populating the $2p_{-1}$ state is increased with an increase of the projectile energy. For small impact parameter domain, the orientation parameters have minima which correspond to the complete $1s \rightarrow 2p_{-1}$ transitions since the $1s \rightarrow 2p_{+1}$ transition probabilities are quite small since the transition matrix elements include the close-encounter effects. The plasma-screening effects on the bound electron in target ion slightly increase the probability of populating the $2p_{-1}$ state. The target screening effects are found to be more important for the case of the small ion-sphere and slightly increased with increasing the projectile energy. Since the line intensity ratios are directly related to the ratio of the $1s \rightarrow 2p_{\pm 1}$ excitation rates, the orientation parameter for the $1s \rightarrow 2p_{\pm 1}$ excitations would be expected to prove the information of the plasma parameter in strongly coupled plasmas. These results provide a general description of the orientation phenomena for *s-p* excitation in strongly coupled plasmas.

The author gratefully acknowledges Prof. R.J. Gould for the warm hospitality at the University of California, San Diego where this work was performed. The author is also grateful to Prof. J.C.Y. Chen for valuable discussions. This work was supported by the Korea Science and Engineering Foundation through Grant No. 981-0205-016-2 and by the Korea Research Foundation through the Basic Science Research Institute Program (1998-015-D00128).

References

1. R.K. Janev, L.P. Presnyakov, V.P. Shevelko, *Physics of Highly Charged Ions* (Springer-Verlag, Berlin, 1985), chapt. 10.
2. Y.-D. Jung, Phys. Plasmas **2**, 332 (1995).
3. Y.-D. Jung, Phys. Plasmas **2**, 1775 (1995).
4. L.G. Dyachkov, *Transport and Optical Properties of Nonideal Plasma*, edited by G.A. Kobzev, I.T. Iakubov, M.M. Popovich (Plenum, New York, 1995), chapt. 5.
5. Y.-D. Jung, Phys. Plasmas **4**, 4254 (1997).
6. Y.-D. Jung, Phys. Plasmas **5**, 536 (1998).
7. M.R.C. McDowell, J.P. Coleman, *Introduction to the Theory of Ion-Atom Collisions* (North-Holland, Amsterdam, 1970), chapt. 4.
8. J.P. Hansen, J.M. Hansteen, J. Phys. B: At. Mol. Opt. Phys. **25**, L183 (1992).
9. N. A. Cherepkov, Adv. Atom. Mol. Phys. **34**, 207 (1994).
10. N. Andersen, D. Dowek, A. Dubois, J.P. Hansen, S.E. Nielsen, Phys. Scripta **42**, 266 (1990).
11. Y.-D. Jung, Phys. Plasmas **2**, 987 (1995).
12. Y.-D. Jung, I.-D. Cho, Phys. Rev. E **52**, 5333 (1995).
13. S. Ichimaru, *Plasma Physics: An Introduction to Statistical Physics of Charged Particles* (Benjamin, Menlo Park, CA, 1986), chapt. 2.
14. E.E. Salpeter, Aust. J. Phys. **7**, 373 (1954).
15. H.R. Greim, *Principles of Plasma Spectroscopy* (Cambridge University Press, Cambridge, 1997), chapt. 7.
16. Y.-D. Jung, Phys. Plasmas **3**, 4376 (1996).
17. Y.-D. Jung, Phys. Plasmas **5**, 779 (1998).
18. Y.-D. Jung, H.-D. Jeong, Phys. Rev. E **54**, 1912 (1996).
19. J.H. McGuire, *Electron Correlation Dynamics in Atomic Collisions* (Cambridge University Press, Cambridge, 1997), chapt. 2.
20. Y.-D. Jung, Phys. Fluids B **5**, 3432 (1993).
21. Y.-D. Jung, Astrophys. J. **409**, 841 (1993).
22. G.B. Arfken, H.J. Weber, *Mathematical Methods for Physicists*, 4th ed. (Academic, San Diego, CA, 1995), p. 749.
23. W. Hong, Y.-D. Jung, Phys. Plasmas **3**, 2457 (1996).
24. H.A. Bethe, R. Jackiw, *Intermediate Quantum Mechanics* (Benjamin, Menlo Park, CA, 1986), chapt. 8.
25. J.-S. Yoon, Y.-D. Jung, Phys. Plasmas **5**, 4461 (1998).